The Performance of a Coherent Residual Carrier PSK System Using Hybrid Carrier Phase Synchronization

M. Simon, H. Tsou, S. Hinedi, and K. Hamdan
Communications Systems and Research Section

This article presents a generic theory for the behavior and performance of hybrid carrier synchronization loops, i.e., loops composed of a combination of discrete and suppressed carrier types, and evaluates their impact on the error probability performance of a phase-shift-keyed (PSK) communication system. Since hybrid loops are characterized by two not necessarily equiprobable lock points (one at zero phase error and one at 180-deg phase error), it is necessary to properly take this phenomenon into account in predicting hybrid loop performance. As such, a new form of solution for the phase error probability density is proposed based on the solution of the Zakai equation. Using this mathematical model, the mean-squared phase error of the hybrid loop is derived and numerically compared with results obtained from a computer simulation. Two methods of resolving the inherent 180-deg phase ambiguity associated with using a hybrid loop for carrier synchronization are discussed, and the corresponding average error probability performances of an associated PSK system are evaluated.

I. Introduction

In the design of many coherent communication systems that transmit data in the form of phase modulation on a carrier, a residual carrier component exists by virtue of the fact that the modulation angle is chosen to be other than 90 deg. Ordinarily in such systems, carrier phase synchronization is achieved by locking a phase-locked loop (PLL) to the residual carrier component of the received signal. Since, however, the residual carrier and data-modulated sidebands are coherently related, it is possible to exploit this coherence to improve the phase synchronization process. The resulting design takes the form of a hybrid carrier tracking loop in that its error signal is a hybrid of those produced by discrete carrier (PLL) and suppressed-carrier (Costas) tracking loops. In fact, it quite easily can be shown that such a closed-loop structure is *motivated* by considering the problem of finding the maximum a posteriori (MAP) estimator of carrier phase for a residual carrier, phase-shift-keyed (PSK) modulated signal. By *motivation* we mean that the error signal in the closed-loop configuration is derived from the derivative of the likelihood function in the neighborhood of the MAP estimate.

The notion of such a hybrid tracking loop was first presented in [1]. However, no performance results were given there, and the discussion was limited to a derivation of the loop equation of operation and equations for the probability density function of the phase error and the nth moment of the first-slip time.

Many years later, an all-digital technique for the coherent demodulation of a residual carrier signal with a biphase modulated square-wave subcarrier was considered [2]. Embedded in this technique was a carrier phase synchronization scheme that exploited the power in the data-bearing signal component as well as that in the residual carrier. In principle, the error signal generated by a Costas loop operating on the subcarrier-demodulated data-bearing signal component was combined with (added to) that generated by a PLL operating on the residual carrier signal component to produce an overall improvement in mean-square phase error performance. In characterizing the performance of such a hybrid loop, the authors of [2] made certain simplifying assumptions that in certain circumstances do not adequately predict this performance. The purpose of this article is to present a generic theory for the behavior and performance of hybrid carrier synchronization loops (the specific configuration suggested in [2] as well as more general forms) and to evaluate their impact on the error probability performance of an associated PSK communication system.

II. Analysis of the Hybrid Loop Operation

Consider the hybrid tracking loop illustrated in Fig. 1 for a residual carrier signal with a biphase-modulated square-wave subcarrier. The mathematical form of the received signal that serves as the input to this loop is

$$r(t) = \sqrt{2P_t}\sin\left(\omega_c t + \theta_m d(t) Sq(\omega_{sc} t)\right) + n(t) \tag{1}$$

where P_t is the total signal power; θ_m is the modulation angle; $d(t)$ is a binary random data waveform with rectangular pulse shape that takes on values ± 1 at the bit rate $1/T_b$; $Sq(\omega_{sc}t)$ is a unit square-wave subcarrier with radian frequency ω_{sc}; ω_c is the carrier radian frequency; and $n(t)$ is additive white Gaussian noise with single-sided power spectral density N_0 W/Hz. In terms of the power in the residual carrier component, $P_c = P_t \cos^2\theta_m$, and the power in the data component, $P_d = P_t \sin^2\theta_m$, by using simple trigonometry, Eq. (1) can be rewritten as

$$r(t) = \sqrt{2P_c}\sin\omega_c t + \sqrt{2P_d} d(t) Sq(\omega_{sc} t)\cos\omega_c t + n(t) \tag{2}$$

Multiplying Eq. (2) by the in-phase (I) and quadrature (Q) reference signals, $r_c(t) = 2\cos(\omega_c t - \phi)$ and $r_s(t) = -2\sin(\omega_c t - \phi)$, respectively, and ignoring terms involving second harmonics of the carrier gives

$$\left.\begin{aligned} \varepsilon_c(t) &= r(t) r_c(t) = \sqrt{2P_c}\sin\phi + \sqrt{2P_d} d(t) Sq(\omega_{sc} t)\cos\phi + 2\cos(\omega_c t - \phi) n(t) \\ \varepsilon_s(t) &= r(t) r_s(t) = -\sqrt{2P_c}\cos\phi + \sqrt{2P_d} d(t) Sq(\omega_{sc} t)\sin\phi + 2\sin(\omega_c t - \phi) n(t) \end{aligned}\right\} \tag{3}$$

where ϕ is the phase error associated with the carrier demodulation process. After multiplication by the square-wave subcarriers[1] and passing through the integrate-and-dump (I&D) filters, we get[2]

$$\left.\begin{aligned} z_c &\triangleq \int_0^{T_b} \varepsilon_c(t) Sq(\omega_{sc} t) dt = \sqrt{2P_d} T_b d_0 \cos\phi + N_c' \\ z_s &\triangleq \int_0^{T_b} \varepsilon_s(t) Sq(\omega_{sc} t) dt = \sqrt{2P_d} T_b d_0 \sin\phi - N_s' \end{aligned}\right\} \tag{4}$$

[1] As mentioned in the introduction, we assume that the subcarrier demodulation is perfect.

[2] For simplicity, we shall assume that the I&D circuits operate on the 0th data bit in the data sequence and, thus, the integration interval extends from 0 to T_b.

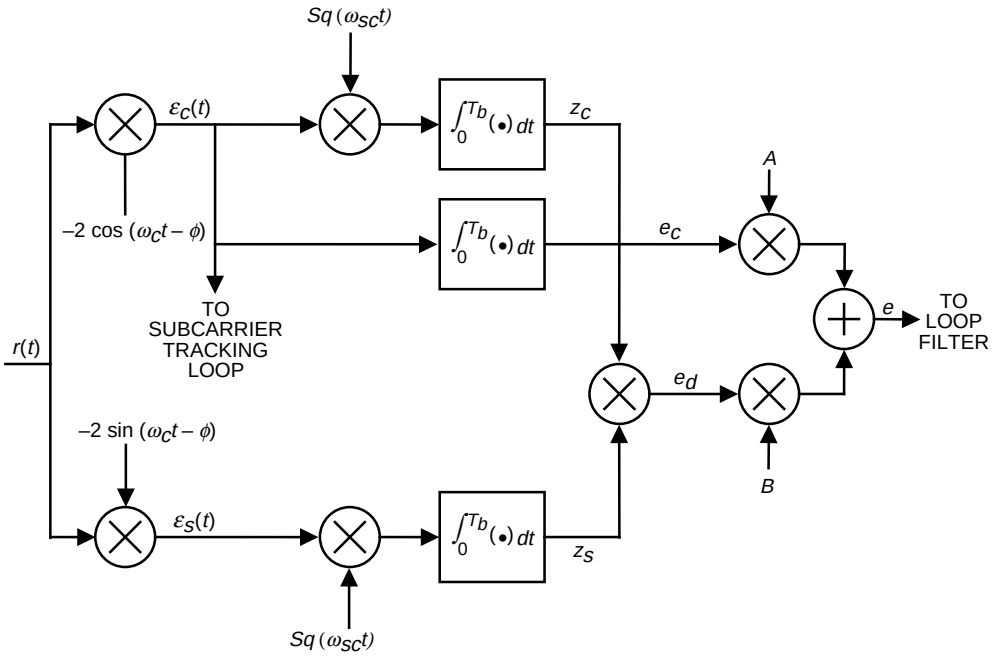

Fig. 1. A hybrid carrier tracking loop for BPSK signals with residual carrier.

where N_c' and N_s' are zero-mean independent Gaussian random variables each with variance $\sigma_n^2 = N_0 T_b$, and d_0 is the 0th data bit in $d(t)$. When multiplied, the signals in Eq. (4) produce the error signal, e_d, in the Costas loop portion of the hybrid loop. In particular,

$$e_d \triangleq z_c z_s = P_d T_b^2 \sin 2\phi + \sqrt{2P_d} T_b d_0 N_c' \sin\phi - \sqrt{2P_d} T_b d_0 N_s' \cos\phi - N_c' N_s' \tag{5}$$

For the error signal of the PLL portion of the hybrid loop, $\varepsilon_c(t)$ is passed through an I&D without being first multiplied by the subcarrier, producing

$$e_c \triangleq \int_0^{T_b} \varepsilon_c(t) dt = \sqrt{2P_c} T_b \sin\phi + N_c \tag{6}$$

where N_c is again a zero-mean Gaussian random variable with variance $\sigma_n^2 = N_0 T_b$. In arriving at Eq. (6), we have made the practical assumption that the subcarrier frequency is either much larger than or an integer multiple of the data rate. Furthermore, using the same assumption, it is straightforward to show that N_c is uncorrelated with N_c' an N_s' under the simplifying assumption that the bit timing clock and the subcarrier are synchronous.

The total error signal is formed from a weighted sum of Eqs. (5) and (6), namely $e = Ae_c + Be_d$. The mean of e is referred to as the loop S-curve and, from Eqs. (5) and (6), is given by

$$g(\phi) = A\sqrt{2P_c} T_b \sin\phi + BP_d T_b^2 \sin 2\phi \tag{7}$$

Depending on the relative values of A and B, the loop can have stable lock points (i.e., $g(\phi) = 0$ with $dg(\phi)/d\phi > 0$) at $\phi = 0$ and $\phi = \pi$. In a fully suppressed carrier loop, these two lock points occur

with equal probability, i.e., the loop is just as likely to lock at $\phi = 0$ as it is to lock at $\phi = \pi$. In the hybrid loop, depending on the relative values of A and B, these two lock points in general will not be equiprobable. Nonetheless, since the lock point at $\phi = 0$ is clearly the desired one (locking at $\phi = \pi$ would result in inverted data), it is essential that this lock point ambiguity be resolved prior to data detection. The simplest (although not necessarily the best from a performance standpoint) way of resolving the above-mentioned 180-deg carrier phase ambiguity is to employ differential encoding. We shall say more about this later on in our discussion of error probability performance.

The slopes of the S-curve at these two lock points are

$$\left.\begin{aligned} K_0 &\triangleq \frac{dg(\phi)}{d\phi}|_{\phi=0} = A\sqrt{2P_c}T_b + 2BP_dT_b^2 \\ K_\pi &\triangleq \frac{dg(\phi)}{d\phi}|_{\phi=\pi} = -A\sqrt{2P_c}T_b + 2BP_dT_b^2 \end{aligned}\right\} \tag{8}$$

Thus, a stable lock point will exist at $\phi = \pi$ (i.e., $K_\pi > 0$) whenever

$$2BP_dT_B^2 > A\sqrt{2P_c}T_b \tag{9}$$

Since the gains A and B are design parameters and should be chosen to optimize system performance (to be discussed shortly), it is quite possible that Condition (9) can be satisfied and, thus, one must take this possibility into account when assessing performance.

The noise component of the total error signal, $N(t)$, is a piecewise constant (over an interval of duration equal to the bit time) random process. In particular, in the interval $T_b \le t \le 2T_b$, this noise process is described by the random variable

$$N = AN_c + B\left[\sqrt{2P_d}T_b d_0\left(N_c' \sin\phi + N_s' \cos\phi\right) - N_c'N_s'\right] \tag{10}$$

When evaluated at $\phi = 0$ and $\phi = \pi$, this random variable has the forms

$$\left.\begin{aligned} N|_{\phi=0} &\triangleq \eta_0 = AN_c + B\left[\sqrt{2P_d}T_b d_0 N_s' - N_c'N_s'\right] \\ N|_{\phi=0} &\triangleq \eta_\pi = AN_c + B\left[-\sqrt{2P_d}T_b d_0 N_s' - N_c'N_s'\right] \end{aligned}\right\} \tag{11}$$

both of which are zero mean and have equal variance, given by

$$\sigma_N^2 = A^2N_0T_b + B^2\left[2P_dT_b^2N_0T_b + (N_0T_b)^2\right] = N_0T_b\left[A^2 + B^2(2P_dT_b^2 + N_0T_b)\right] \tag{12}$$

The autocorrelation function of the piecewise constant noise process $N(t)$ is a triangular function with height σ_N^2 and width $2T_b$. For a narrowband loop, i.e., one whose single-sided loop bandwidth, B_L, is much smaller than the data rate, one can approximate $N(t)$ as a delta-correlated process [3] with a flat single-sided power spectral density, $N_0' = 2\sigma_n^2T_b$.

Finally, assuming that the hybrid loop of Fig. 1 is closed using a loop filter with transfer function $F(s)$ and a voltage-controlled oscillator (VCO) with transfer function K/s, then the stochastic differential equation describing the operation of the loop is

$$\dot{\phi} = \dot{\theta} - KF(p)e = \dot{\theta} - KF(p)\left(A\sqrt{2P_c}T_b \sin\phi(t) + BP_dT_b^2 \sin 2\phi(t) + N(t)\right) \tag{13}$$

where the dot denotes differentiation with respect to time and p is the Heaviside operator.

III. Mean-Square Phase Error Performance in the Linear Region of Loop Operation

In the linear region of loop operation, i.e., where the loop S-curve of Eq. (7) can be approximated by the linear function $K_0\phi$ or $K_\pi(\phi - \pi)$, the conditional mean-square phase error (the conditioning is on the loop locking at $\phi_l = 0$ or π) is computed as

$$\sigma_\phi^2|_{\phi_l=0 \text{ or } \pi} = \frac{N_0' B_{L\phi_l}}{K_{\phi_l}^2} \tag{14}$$

Here, $B_{L\phi_l}$ denotes the single-sided loop bandwidth that depends on whether the loop is locked at $\phi_l = 0$ or π rad. The reason for this distinction is that the linear loop bandwidth is dependent on the total loop gain, which includes as one of its components the slope of the S-curve that, from Eq. (8), is different for the two lock points. Since, depending on which of the two lock points the loop locks to, K_{ϕ_l} assumes either the value K_0 or the value K_π of Eq. (8), then, from Eq. (12), $\sigma_\phi^2|_{\phi_l=0 \text{ or } \pi}$ evaluates to

$$\sigma_\phi^2|_{\phi_l=0 \text{ or } \pi} = \left(\frac{N_0 B_{L\phi_l}}{P_c}\right) \frac{\left[1 + \gamma^2(2P_dT_b^2 + N_0T_b)\right]}{\left(1 \pm \gamma\dfrac{2P_d}{\sqrt{2P_c}}T_b\right)^2} \triangleq \left(\frac{N_0 B_{L\phi_l}}{P_c}\right) L_{\phi_l}^{-1} \tag{15}$$

where $\gamma \triangleq B/A$ is the ratio of the gains[3] in the two arms of the hybrid loop that contribute to the total error signal, where the plus sign in the denominator is associated with the lock point at $\phi_l = 0$ and the minus sign is associated with the lock point at $\phi_l = \pi$. Also, in Eq. (15), L_{ϕ_l} is a *loop performance parameter* that represents the behavior of the mean-square phase error of the hybrid loop relative to that of a conventional PLL.

The *conditional effective loop signal-to-noise ratio* (SNR) of the hybrid loop, $\rho_{eff}|_{\phi_l=0 \text{ or } \pi}$, is defined as the reciprocal of Eq. (15). Note that when $\gamma = 0$, i.e., only the discrete carrier component of the input signal contributes to the hybrid loop error signal, there is no lock point at $\phi = \pi$ and $\rho_{eff}|_{\phi_l=0} = \rho_{PLL}$, where $\rho_{PLL} \triangleq P_c/N_0B_{L0}$ is the loop SNR of a PLL. At the other extreme, when $\gamma = \infty$, i.e., only the suppressed carrier component of the input signal contributes to the hybrid loop error signal, in which case equiprobable lock points occur at $\phi = 0, \pi$ and

[3] Note from Condition (9) that γ is not dimensionless. In particular, it has units of (volt-sec)$^{-1}$.

$$\left.\begin{aligned} \rho_{eff}|_{\phi_l=0,\pi} &= \left(\frac{P_d}{N_0 B_{L0}}\right)\left[\frac{2R_d}{2R_d+1}\right] \triangleq \frac{P_d}{N_0 B_{L0}} S_L = \rho_{Costas} \\ R_d &= \frac{P_d T_b}{N_0} \\ B_{L0} &= B_{L\pi} \end{aligned}\right\} \tag{16}$$

which is precisely what one would obtain by tracking a suppressed carrier signal with power P_d using an I–Q Costas loop [3]. In Eq. (16), S_L denotes the squaring loss of the I–Q Costas loop [3] that results from the presence of signal-times-noise ($S \times N$) and noise-times-noise ($N \times N$) components in the loop error signal [see Eq. (5)].

From the standpoint of phase tracking, it is desirable to choose γ so as to minimize $\sigma_\phi^2|_{\phi_l=0 \text{ or } \pi}$ of Eq. (15) or equivalently to maximize $\rho_{eff}|_{\phi_l=0 \text{ or } \pi}$. Assuming that the loop locks at $\phi = 0$ (the desired lock point), i.e., the plus sign in the denominator of Eq. (15), then differentiating L_0 with respect to γ and equating the result to zero results in

$$\gamma_{opt}|_{\phi_l=0} \triangleq \gamma_{opt_0} = \left(\sqrt{2P_c}T_b\right)^{-1} S_L \tag{17}$$

Substituting Eq. (17) into Eq. (15) gives

$$\rho_{eff}|_{\phi_l=0} \triangleq \rho_0 = \left(\frac{P_c}{N_0 B_{L0}}\right)\left(1 + \frac{P_d}{P_c} S_L\right) = \frac{P_c}{N_0 B_{L0}} + \frac{P_d}{N_0 B_{L0}} S_L \triangleq \rho_{PLL} + \rho_{Costas} \tag{18}$$

This result corresponds to the performance measure used in [2].

With the gain ratio chosen as in Eq. (17), if the loop were to lock at $\phi = \pi$, then the effective loop SNR would be

$$\rho_{eff}|_{\phi_l=\pi} \triangleq \rho_\pi = \left(\frac{P_c}{N_0 B_{L\pi}}\right)\left(-1 + \frac{P_d S_L}{P_c}\right)^2 \left(1 + \frac{P_d S_L}{P_c}\right)^{-1} \tag{19}$$

Also note that with the gain ratio chosen as in Eq. (17), the condition for the existence of a stable lock point at $\phi = \pi$, as given in Condition (9), becomes

$$\frac{P_c}{P_d} = \cot^2\theta_m < S_L \rightarrow \tan\theta_M > \sqrt{\frac{2R_d+1}{2R_d}} \tag{20}$$

or, in terms of the component loop SNRs,

$$\rho_{PLL} < \rho_{Costas} \tag{21}$$

Had we elected to optimize the gain ratio based on the assumption that the loop locks at $\phi = \pi$, then the optimum value of γ would be the negative of Eq. (17) and the results in Eqs. (18) and (19) would simply switch with each other.

The average mean-square phase error performance of the loop in the linear region of operation can be computed from Eq. (14) as

$$\sigma_\phi^2 = P_0\sigma_\phi^2|_{\phi_l=0} + P_\pi\sigma_\phi^2|_{\phi_l=\pi} \triangleq P_0\sigma_0^2 + P_\pi\sigma_\pi^2 \tag{22}$$

where P_0 and P_π respectively denote the probabilities that the loops lock at the two possible loop lock points, $\sigma_l = 0$ and $\sigma_l = \pi$.[4] For the optimum gain ratio of Eq. (17), i.e., that which minimizes σ_0^2, the average mean-square phase error of Eq. (22) would be evaluated as

$$\sigma_\pi^2 = P_0\left(\frac{P_c}{N_0B_{L0}}\right)^{-1}\left(1+S_L\tan^2\theta_m\right)^{-1} + P_\pi\left(\frac{P_c}{N_0B_{L\pi}}\right)^{-1}\left[\frac{\left(-1+S_L\tan^2\theta_m\right)^2}{\left(1+S_L\tan^2\theta_m\right)}\right]^{-1} \tag{23}$$

For a first-order loop, i.e., $F(s) = 1$, we would have

$$\left.\begin{aligned} B_{L0} &= \frac{K_0K}{4} \\ B_{L\pi} &= \frac{K_\pi K}{4} \end{aligned}\right\} \tag{24}$$

where K_0 and K_π are defined in Eq. (8). Thus, Eq. (23) can be written alternatively as

$$\sigma_\phi^2 = P_0\left(\frac{P_c}{N_0B_{L0}}\right)^{-1}\left(1+S_L\tan^2\theta_m\right)^{-1} + P_\pi\left(\frac{P_c}{N_0B_{L0}}\right)^{-1}\left(-1+S_L\tan^2\theta_m\right)^{-1} \tag{25}$$

The (unconditional) effective loop SNR of the hybrid loop, ρ_{eff}, is defined as the reciprocal of Eq. (25). What remains is to evaluate P_0 and P_π. Before performing these evaluations, however, we first must characterize the probability density function (pdf) of the phase error in the nonlinear region of operation and its behavior in the linear region around the two lock points.

IV. Probability Density Function of the Loop Phase Error

For the stochastic differential equation of Eq. (13) and for a first-order loop (also approximately for a second-order loop), the unconditional pdf of the phase error $p(\phi)$ (i.e., the solution to the steady-state Fokker–Planck equation) is given by[5]

$$p(\phi) = C\exp\left\{-\left(\frac{K_0^2}{N_0'B_{L0}}\right)\int g_n(\phi)d\phi\right\} \tag{26}$$

where we have normalized the loop S-curve of Eq. (7) in terms of a unit slope (at $\phi = 0$) nonlinearity, i.e., $g(\phi) \triangleq K_0g_n(\phi)$ with K_0 as defined in Eq. (8), and C is a normalization constant chosen to assure that $p(\phi)$ has unit area over the interval $-\pi \le \phi \le \pi$. Using Eqs. (7) and (8) and the optimum gain ratio of Eq. (17) in Eq. (26), we get

[4] Later on we shall discuss how P_0 and P_π can be evaluated.

[5] The generic form of Eq. (18), which applies to a synchronous control loop, can be found in [5].

$$p(\phi) = C \exp\left\{\left(\frac{P_c}{N_0 B_{L0}}\right)\left(\cos\phi + 0.25 S_L \tan^2\theta_m \cos 2\phi\right)\right\}$$

$$= C \exp\left\{\rho_{PLL}\cos\phi + 0.25\rho_{Costas}\cos 2\phi\right\}, \quad |\phi| \le \pi \tag{27}$$

This then represents the pdf of the loop phase error when the loop is optimized to maximize ρ_{eff} corresponding to a locked state at $\phi = 0$. When Condition (9) is satisfied, i.e., a stable lock point exists at $\phi = \pi$, then the pdf of Eq. (27) will be bimodal.

Under the appropriate conditions (see the Appendix), the pdf of Eq. (27) also can be expressed as a weighted sum of two conditional pdf's, $p_0(\phi)$ and $p_\pi(\phi)$, each distributed on the interval $-\pi \le \phi \le \pi$, which respectively represent the pdf of the loop phase error ϕ conditioned on the two possible loop lock points $\phi_l = 0$ and $\phi_l = \pi$. The appropriate representation is

$$p(\phi) = P_0 p_0(\phi) + P_\pi p_\pi(\phi) \tag{28}$$

where P_0 and P_π are as previously defined. Unfortunately, one cannot obtain $p_0(\phi)$ and $p_\pi(\phi)$ by direct decomposition of Eq. (27). Rather, these conditional pdf's are obtained by numerical solution of the Zakai equation [6], which is the Fokker–Planck equation augmented with a term dependent on the observation (i.e., at which lock point the loop is located). The values of P_0 and P_π are also found from this approach. The procedure is discussed in the Appendix and in more detail in Hamdan et al.[6]

V. Evaluation of P_0 and P_π in the Linear Region of Operation

In the linear region where the effective loop SNR is large, the modes of Eq. (28) around $\phi = 0$ and $\phi = \pi$ will tend toward Gaussian functions that, for all practical purposes, are nonoverlapping and thus, to a good approximation, the mode around $\phi = 0$ will correspond to $P_0 p_0(\phi)$ and the mode around $\phi = \pi$ will correspond to $P_\pi p_\pi(\phi)$. Assuming a hybrid loop whose gain ratio γ has been chosen to optimize performance around $\phi = 0$, then expanding the argument of the exponential in Eq. (27) around $\phi = 0$ gives

$$P_0 p_0(\phi) \simeq C \exp\left\{\rho_{PLL}\left(1 + 0.25 S_L \tan^2\theta_m\right)\right\} \exp\left(-\frac{\theta^2}{2\sigma_0^2}\right) \tag{29}$$

where

$$\sigma_0^2 \triangleq \left[\rho_{PLL}\left(1 + S_L \tan^2\theta_m\right)\right]^{-1} \tag{30}$$

Similarly, expanding the argument of the exponential in Eq. (27) around $\phi = \pi$ gives

$$P_\pi p_\pi(\phi) \simeq C \exp\left\{\rho_{PLL}\left(-1 + 0.25 S_L \tan^2\theta_m\right)\right\} \exp\left(-\frac{(\phi - \pi)^2}{2\sigma_\pi^2}\right) \tag{31}$$

where

[6] K. Hamdan, S. Hinedi, and M. Simon, "The Steady State Behavior of Randomly Perturbed Dynamical Systems Near Stable Equilibria," submitted to *IEEE Transactions on Information Theory*.

$$\sigma_\pi^2 \triangleq \left[\rho_{PLL}\left(-1+S_L\tan^2\theta_m\right)\right]^{-1} \tag{32}$$

To evaluate the normalization constant C, we make use of Eq. (21), in which case

$$\begin{aligned} 1 &= \int_{-\pi}^{\pi} p(\phi)d\phi \simeq \int_{-\infty}^{\infty} P_0 p_0(\phi)d\phi + \int_{-\infty}^{\infty} P_\pi p_\pi(\phi)d\phi \\ &= C\left[\sqrt{2\pi\sigma_0^2}\exp\left\{\rho_{PLL}(1+0.25S_L\tan^2\theta_m)\right\} + \sqrt{2\pi\sigma_\pi^2}\exp\left\{\rho_{PLL}(-1+0.25S_L\tan^2\theta_m)\right\}\right] \end{aligned} \tag{33}$$

or

$$C = \left[\sqrt{2\pi}\exp\left\{0.25\rho_{PLL}S_L\tan^2\theta_m\right\}\left(\sigma_0\exp\{\rho_{PLL}\} + \sigma_\pi\exp\{-\rho_{PLL}\}\right)\right]^{-1} \tag{34}$$

Combining Eqs. (29) and (31) gives

$$\left.\begin{aligned} P_0 p_0(\phi) &\simeq \left[1+\left(\frac{\sigma_\pi}{\sigma_0}\right)\exp(-2\rho_{PLL})\right]^{-1}\frac{\exp\left(-\dfrac{\phi^2}{2\sigma_0^2}\right)}{\sqrt{2\pi\sigma_0^2}} \\ P_\pi p_\pi(\phi) &\simeq \left[1+\left(\frac{\sigma_\pi}{\sigma_0}\right)\exp(2\rho_{PLL})\right]^{-1}\frac{\exp\left(-\dfrac{(\phi-\pi)^2}{2\sigma_\pi^2}\right)}{\sqrt{2\pi\sigma_\pi^2}} \end{aligned}\right\} \tag{35}$$

Had we linearized the loop equation of Eq. (13) around $\phi = 0$ by setting $\sin\phi = \phi$ and $\sin 2\phi = 2\phi$ right from the start, then the steady-state solution for the pdf $p(\phi)$ would be precisely

$$p(\phi) = p_0(\phi) = \frac{\exp\left(-\dfrac{\phi^2}{2\sigma_0^2}\right)}{\sqrt{2\pi\sigma_0^2}} \tag{36}$$

Similarly, had we linearized the loop equation of Eq. (13) around $\phi = \pi$ by setting $\sin\phi = \phi - \pi$ and $\sin 2\phi = 2(\phi-\pi)$ right from the start, then the steady-state solution for the pdf $p(\phi)$ would be precisely

$$p(\phi) = p_\pi(\phi) = \frac{\exp\left(-\dfrac{(|\phi|-\pi)^2}{2\sigma_\pi^2}\right)}{\sqrt{2\pi\sigma_\pi^2}} \tag{37}$$

Thus, comparing Eqs. (36) and (37) with Eq. (35) gives the desired results,

$$\left.\begin{aligned} P_0 &= \left[1+\left(\frac{\sigma_\pi}{\sigma_0}\right)\exp(-2\rho_{PLL})\right]^{-1} \\ P_\pi &= \left[1+\left(\frac{\sigma_0}{\sigma_\pi}\right)\exp(2\rho_{PLL})\right]^{-1} \end{aligned}\right\} \tag{38}$$

or, using Eqs. (30) and (32),

$$\left.\begin{aligned} P_0 &= \left[1+\sqrt{\frac{1+S_L\tan^2\theta_m}{-1+S_L\tan^2\theta_m}}\exp\left(-\frac{2P_c}{N_0B_{L0}}\right)\right]^{-1} \\ P_\pi &= \left[1+\sqrt{\frac{-1+S_L\tan^2\theta_m}{1+S_L\tan^2\theta_m}}\exp\left(\frac{2P_c}{N_0B_{L0}}\right)\right]^{-1} \end{aligned}\right\} \tag{39}$$

Note from Eq. (39) that $P_0 + P_\pi = 1$, as should be the case.

Figures 2(a) and 2(b) are plots of P_0, as determined from Eq. (39), versus P_t/N_0 in dB-Hz for fixed values of θ_m and B_{L0} and a data rate of $1/T_b$. In terms of these parameters, the loop SNR P_c/N_0B_{L0} and squaring loss S_L are obtained from

$$\left.\begin{aligned} S_L &= \frac{2R_d}{1+2R_d} \\ R_d &= \left(\frac{P_t}{N_0}\right)\left(\frac{1}{T_b}\right)^{-1}\sin^2\theta_m \\ \frac{P_c}{N_0B_{L0}} &= \left(\frac{P_t}{N_0}\right)\left(\frac{1}{B_{L0}}\right)\cos^2\theta_m \end{aligned}\right\} \tag{40}$$

Shown in Table 1 is a comparison of numerical results for P_0 and P_π obtained from the approach taken in the Appendix with those obtained from the linear approach as given in Eq. (39). We observe that, for the three sets of parameters selected for the comparison [which are particular cases of those used to obtain Figs. 2(a) and 2(b)], there is reasonable agreement between the values of P_0 and P_π obtained from the two different approaches. The discrepancy that exists can be attributed to the fact that the assumption of linear region of operation is not completely justified for the parameter sets chosen. Also note that the values of P_0 and P_π obtained from the approach in the Appendix do not precisely sum to unity because of the limitation in the accuracy associated with the numerical solution of the Zakai equation.

Figures 3(a) through 3(c) illustrate the behavior of the pdf $p(\phi)$ as the loop SNR varies from high to low values. Four sets of results are shown in each of these figures. The first set of results is based on the decomposition given in Eq. (28), where the conditional pdf's and the probability weights P_0 and P_π are obtained from the approach taken in the Appendix. The second set of results corresponds to the same decomposition, but the conditional pdf's and probability weights P_0 and P_π are obtained from the linear region approximations given in this section, in particular Eqs. (36) through (39). The third set of results corresponds to the Fokker–Planck solution given in Eq. (27). Finally, as a check on the validity of the analytical models, results obtained from a computer simulation of the actual hybrid loop of Fig. 1 are superimposed on the previous three sets of analytical results.[7]

[7] In the case of Fig. 3(c), simulation results could not be obtained, since the loop had difficulty maintaining lock at such a low loop SNR.

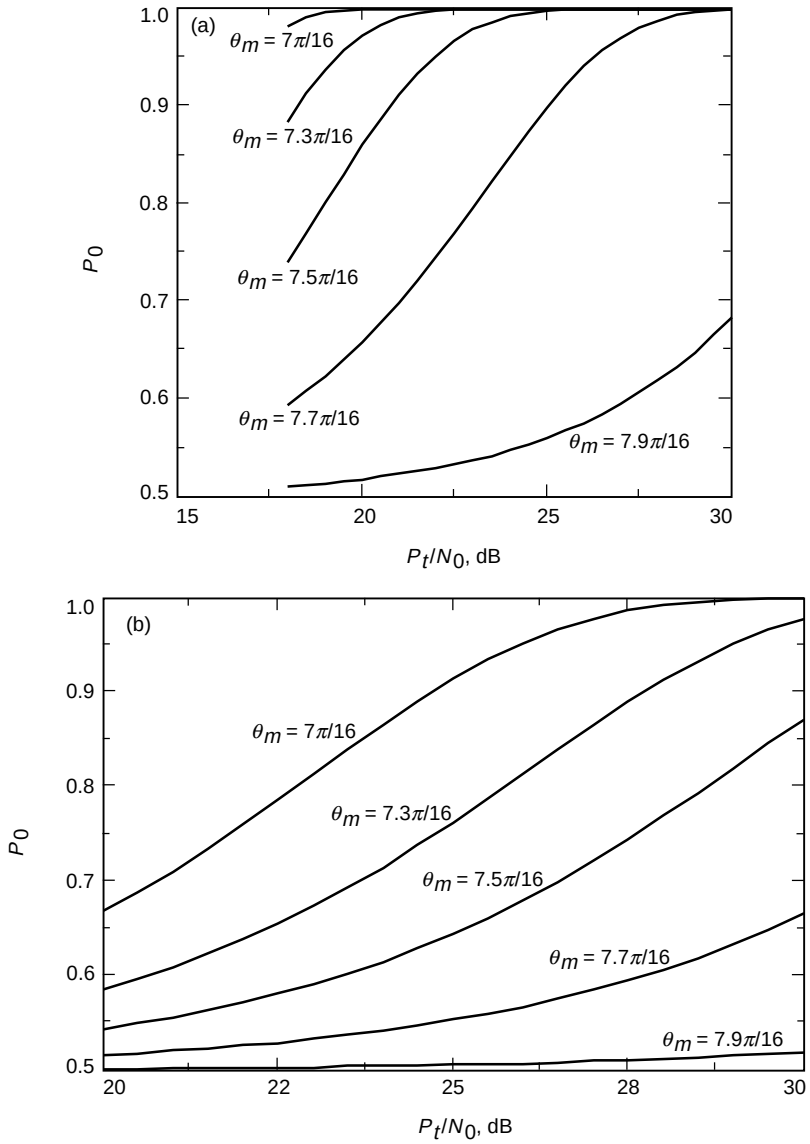

Fig. 2. The probability of locking at ϕ = 0 versus total power-to-noise ratio with modulation angle as a parameter, linear region of operation: (a) B_{L0} = 1 Hz, $1/T_b$ = 2 kHz and (b) B_{L0} = 10 Hz, $1/T_b$ = 100 Hz.

VI. Mean-Square Phase Error Performance in the Nonlinear Region of Loop Operation

To assess the mean-square phase error performance of the loop in the nonlinear region of operation, it is necessary to determine the conditional pdf's of the loop phase error, ϕ, conditioned on the two possible loop lock points, $\phi_l = 0$ and $\phi_l = \pi$, namely, $p_0(\phi)$ and $p_\pi(\phi)$. Once these have been found, then the average mean-square phase error in the nonlinear region of loop operation is given by

$$\sigma_\phi^2 = P_0 \int_{-\pi}^{\pi} \phi^2 p_0(\phi) d\phi + P_\pi \int_{-\pi}^{\pi} (|\phi| - \pi)^2 \, p_\pi(\phi) d\phi \triangleq P_0 \sigma_0^2 + P_\pi \sigma_\pi^2 \tag{41}$$

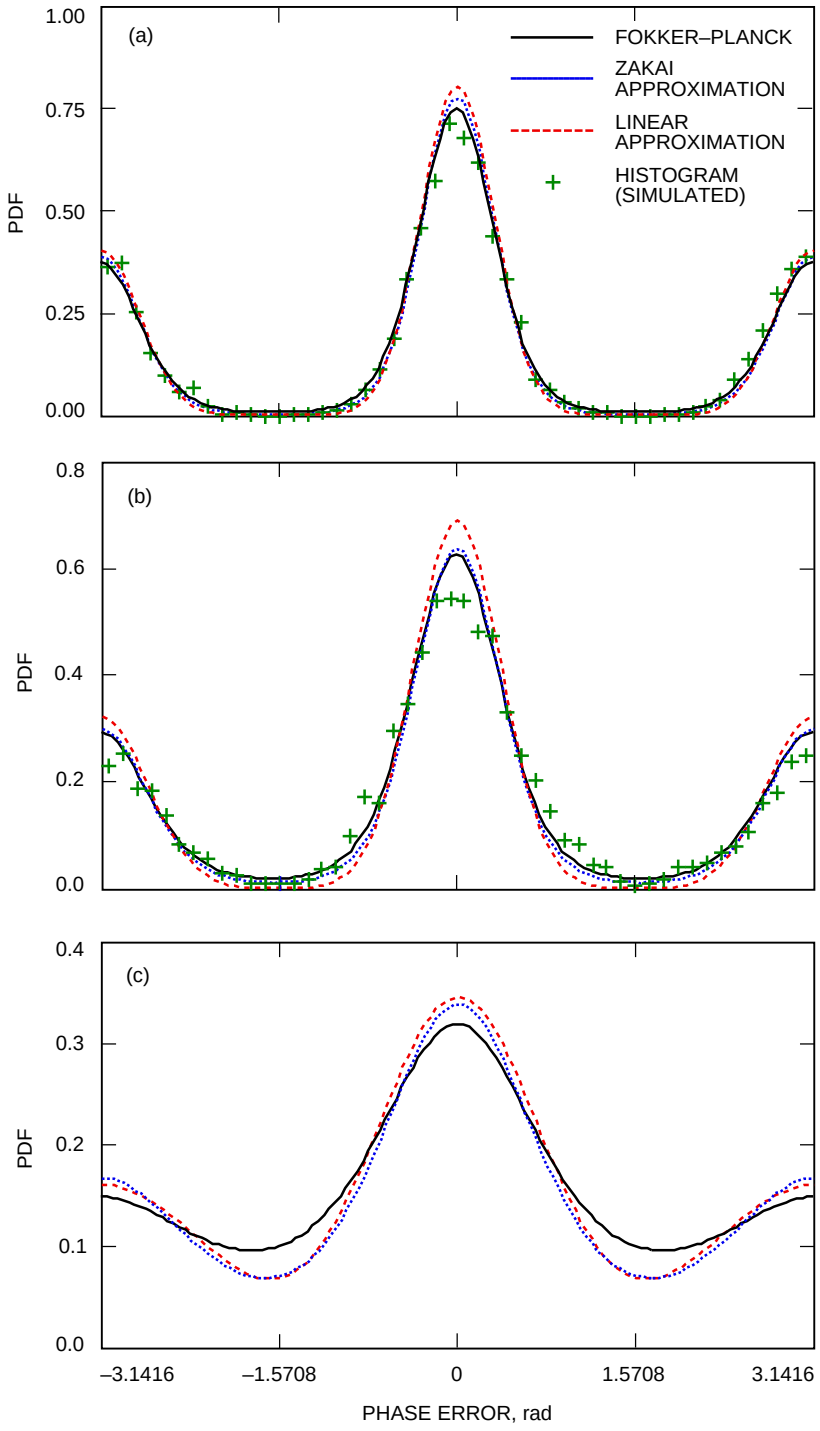

Fig. 3. A comparison of the phase error probability density functions based on linear and nonlinear theories: (a) B_{L0} = 1 Hz, $1/T_b$ = 2 kHz, P_t/N_0 = 20 dB-Hz, $\theta_m = 7.7\pi/16$; (b) B_{L0} = 10 Hz, $1/T_b$ = 100 Hz, P_t/N_0 = 20 dB-Hz, $\theta_m = 7\pi/16$; and (c) B_{L0} = 10 Hz, $1/T_b$ = 1000 Hz, P_t/N_0 = 20 dB-Hz, $\theta_m = 7\pi/16$.

Table 1. A comparison of the probabilities of locking at $\phi = 0$ and $\phi = \pi$ based on linear and nonlinear theories.

Parameter set	$P_0\|_{linear}$	$P_\pi\|_{linear}$	$P_0\|_{Zakai}$	$P_\pi\|_{Zakai}$
$B_{L0} = 1$ Hz $1/T_b = 2$ kbps $P_t/N_0 = 20$ dB-Hz $\theta_m = 7.7\pi/16$ ($\rho_{eff} = 9.604$ dB)	0.658082	0.341918	0.644724	0.321096
$B_{L0} = 10$ Hz $1/T_b = 100$ bps $P_t/N_0 = 20$ dB-Hz $\theta_m = 7\pi/16$ ($\rho_{eff} = 8.087$ dB)	0.668409	0.331591	0.650	0.316
$B_{L0} = 10$ Hz $1/T_b = 1$ kbps $P_t/N_0 = 20$ dB-Hz $\theta_m = 7\pi/16$ ($\rho_{eff} = 1.91453$ dB)	0.625013	0.374987	0.61186	0.34433

Implicit in Eq. (41) is the assumption that the receiver is able to determine when the loop is locked correctly at zero phase error and when it is incorrectly locked at π rad. As suggested in the introduction, a means of accomplishing this is to periodically employ a synchronization word in the data stream to detect when the data have been inverted. Also, in the limit of large SNR where σ_0^2 and σ_π^2 are given by Eqs. (30) and (32), respectively, Eq. (41) gives the same result as Eq. (22).

Although Eq. (41) represents the behavior of the loop in the nonlinear region of operation, it is convenient to define an *effective average loop SNR*, ρ_{ave}, equal to the reciprocal of σ_ϕ^2, which is analogous to what was done in the linear region. In general, ρ_{ave} defined this way will be smaller than ρ_{eff} based on the linear loop analysis, i.e., the reciprocal of Eq. (22).

For the sets of parameter values corresponding to Figs. 3(a) and 3(b), Table 2 compares ρ_{ave} obtained from Eq. (41) with numerical results obtained from a computer simulation of the loop as well as with several different loop SNRs, in particular, ρ_{PLL}, ρ_{Costas}, ρ_0 [see Eq. (18)], and ρ_{eff} [see the reciprocal of Eq. (25)]. In the case of the simulation, the values are obtained by measuring the mean-square phase error and then taking its reciprocal. We observe that the simulation results agree best with ρ_{ave}, as one would expect. Also, we remind the reader that the values of ρ_0 given in the table would be those obtained from the results reported in [2].

VII. Error Probability Performance

A. Phase Ambiguity Resolution Using Differential Encoding/Decoding

One method of resolving the 180-deg ambiguity associated with the hybrid tracking loop locking at π rad is to use a combination of differential encoding and differential decoding, as is done for conventional Costas loops that exhibit the same phase ambiguity. For a binary phase-shift-keyed (BPSK) system with differential encoding/decoding, the conditional (on the phase error) bit-error probability is given by [4]

$$P_b(E;\phi) = \text{ erfc}\left(\sqrt{R_d}\cos\phi\right)\left[1 - 0.5\text{ erfc}\left(\sqrt{R_d}\cos\phi\right)\right] \tag{42}$$

Table 2. A comparison of loop SNRs.

Parameter set	ρ_{ave}, dB [reciprocal of Eq. (41)]	$\rho_{simulation}$, dB [reciprocal of measured σ_ϕ^2]	ρ_{PLL}, dB [Eq. (18)]	ρ_{Costas}, dB [Eq. (18)]	$\rho_0 = \rho_{PLL}$ $+\rho_{Costas}$, dB [Eq. (18)]	ρ_{eff}, dB [reciprocal of Eq. (25)]
$B_{L0} = 1$ Hz $1/T_b = 2$ kbps $P_t/N_0 = 20$ dB-Hz $\theta_m = 7.7\pi/16$	8.247	8.447	−4.602	9.557	9.721	9.604
$B_{L0} = 10$ Hz $1/T_b = 100$ bps $P_t/N_0 = 20$ dB-Hz $\theta_m = 7\pi/16$	5.881	6.180	−4.195	8.014	8.267	8.087

where erfc x denotes the complementary error function with argument x. Note that

$$P_b(E;\phi) = P_b(E;\phi+\pi) \tag{43}$$

which clearly identifies the fact that the 180-deg ambiguity has been resolved, i.e., it is not necessary for the receiver to determine when the loop is locked at $\phi = 0$ and when it is locked at $\phi = \pi$. Stated another way, since

$$P_b\left(E;\frac{\pi}{2}+\phi\right) = P_b\left(E;\frac{\pi}{2}-\phi\right), \quad 0 \le \phi \le \frac{\pi}{2} \tag{44}$$

and since $P_b(E;\phi) \le 0.5$ for $0 \le \phi \le \pi/2$, we see that the conditional error probability can never exceed 0.5 in the interval $-\pi \le \phi \le \pi$. In other words, by folding the conditional error probability around 0.5 at $\phi = \pi/2$, the differential encoding/decoding operation circumvents the need to detect the 180-deg ambiguity and invert the detected data. Despite the fact that the ambiguity has been resolved, the average error probability performance depends on the behaviors of the loop in the neighborhoods of both lock points, which, as we have seen from previous discussions, are different. In particular, the average bit-error probability is computed by averaging Eq. (42) over the pdf in Eq. (27), namely,

$$P_b(E) = \int_{-\pi}^{\pi} P_b(E;\phi)p(\phi)d\phi \tag{45}$$

which, in view of Eq. (43), is equivalent to

$$P_b(E) = \int_{-\pi/2}^{\pi/2} P_b(E;\phi)(p(\phi)+p(\phi+\pi))d\phi \tag{46}$$

Note that when $\theta_m = 90$ deg, i.e., $P_c = 0(\rho_{PLL} = 0)$, then from Eq. (27), $p(\phi) = p(\phi+\pi)$ and Eq. (46) simplifies to

$$P_b(E) = 2\int_{-\pi/2}^{\pi/2} P_b(E;\phi)p(\phi)d\phi \tag{47}$$

which is a well-known result for average error probability performance of BPSK systems employing suppressed-carrier tracking.

The average error probability as computed from Eq. (45) depends on three parameters, namely, R_d, ρ_{PLL}, and ρ_{Costas}. These parameters can in turn be related to the modulation angle, θ_m; the total power-to-noise ratio, P_t/N_0; the data rate, $1/T_b$; and the loop bandwidth, B_{L0}, via

$$\left.\begin{aligned} R_d &= \left(\frac{P_t T_b}{N_0}\right)\sin^2\theta_m \\ \rho_{PLL} &= \left(\frac{P_t}{N_0 B_{L0}}\right)\cos^2\theta_m \\ \rho_{Costas} &= \left(\frac{P_t}{N_0 B_{L0}}\right) S_L \sin^2\theta_m \end{aligned}\right\} \tag{48}$$

Figure 4 is a plot of $P_b(E)$ versus θ_m for $B_{L0} = 1$ Hz, $1/T_b = 100$ bps, and two values of P_t/N_0, namely, 25 and 30 dB-Hz. We observe that, from the standpoint of minimizing average bit-error probability, the optimum *choice* of modulation angle is $\theta_m = 90$ deg, i.e., *suppressed-carrier tracking with an I–Q Costas loop*. We remind the reader that this conclusion is based on designing (optimizing) the hybrid loop to minimize mean-square phase error at the desired lock point, $\phi = 0$.

Suppose that instead we were to design the loop (i.e., choose the gain ratio, γ) to directly minimize the average bit-error probability performance of the receiver. To see how this is done, we first rewrite the pdf of the loop phase error in terms of this gain ratio rather than in the form of Eq. (27), which assumes the optimum γ of Eq. (17). In particular, using Eq. (26) together with Eqs. (8) and (12), we get

$$p(\phi) = C\exp\left\{\rho_{PLL}\left(\frac{1+\gamma'\tan^2\theta_m S_L}{1+\gamma'^2\tan^2\theta_m S_L}\right)\left(\cos\phi + 0.25\gamma'\tan^2\theta_m S_L\cos 2\phi\right)\right\}, \quad |\phi| \le \pi \tag{49}$$

where we have normalized the gain ratio as

$$\gamma' \triangleq \gamma\left(\frac{\sqrt{2P_c}T_b}{S_L}\right) \tag{50}$$

Note that, in accordance with Eq. (17), choosing $\gamma' = 1$ for each value of θ_m would result in the same error-probability performance as shown in Fig. 4. Figure 5 is a plot of average bit-error probability versus γ' for several values of θ_m between 0 and $\pi/2$ for $B_L = 10$ Hz, $1/T_b$ =10 bps, and $P_t/N_0 = 20$ dB-Hz. We observe that, in each case, the optimum (in the sense of minimum error probability) value of γ' is equal or very close to unity. Thus, for all practical purposes, the choice of hybrid loop gains to optimize average bit-error probability performance is the same as that corresponding to minimum mean-square phase error at the correct lock point. This result is not at all obvious at the outset due to the fact that the average error-probability performance depends on the loop performance both in the region around $\phi = 0$ and around $\phi = \pi$. We also observe from Fig. 5 that the sensitivity (or lack thereof) of the error-probability performance to the optimum choice of γ' shifts as θ_m varies between 0 and $\pi/2$. In particular, for small values of θ_m, the performance is virtually insensitive to values of $\gamma' < \gamma'_{opt}$, whereas for large values of θ_m, the same insensitivity occurs for values of $\gamma' > \gamma'_{opt}$.

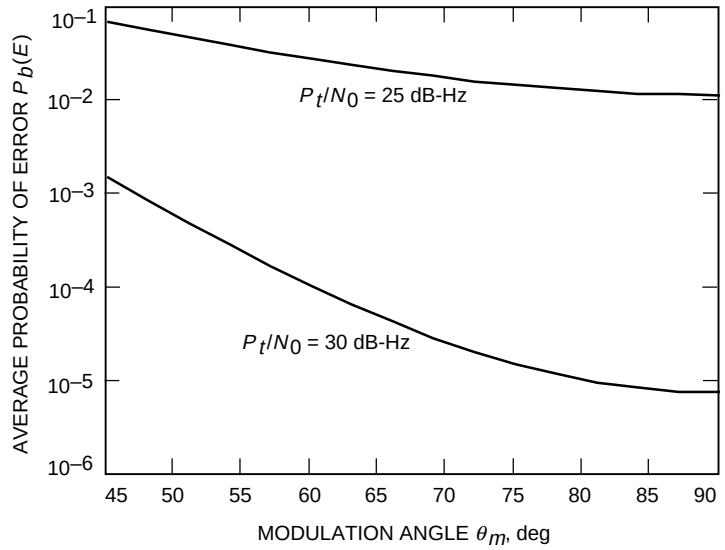

Fig. 4. The error probability performance as a function of the modulation angle, θ_m, with the phase ambiguity resolution provided by differential encoding/decoding, with B_{L0} = 1 Hz, $1/T_b$ = 100 bps, P_t/N_0 = 25, 30 dB-Hz

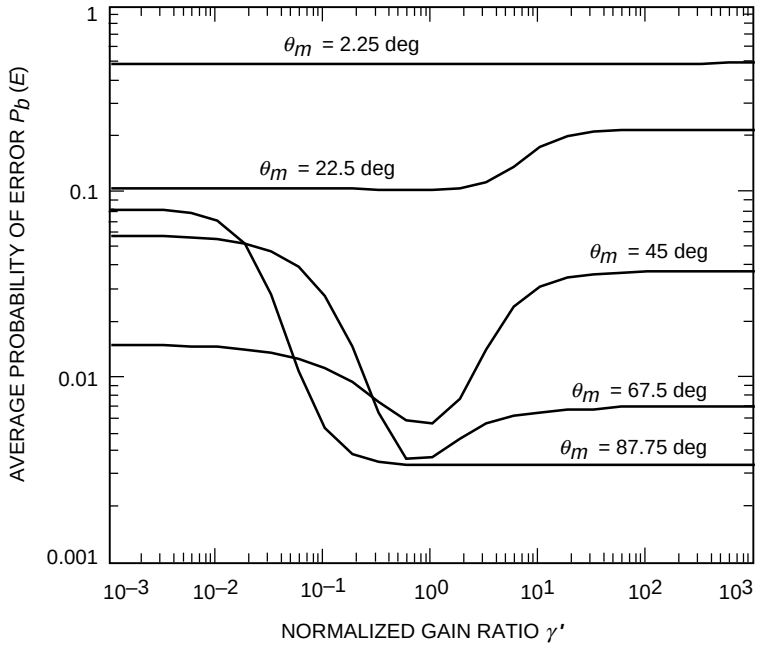

Fig. 5. The error probability performance as a function of the normalized gain ratio, γ', with the modulation angle, θ_m, as a parameter, with B_{L0} = 10 Hz, $1/T_b$ = 10 bps, P_t/N_0 = 20 dB-Hz.

B. Phase Ambiguity Resolution Using a Synchronization Word

Here we assume that the receiver is able to determine when the loop is correctly locked at zero phase error and when it is incorrectly locked at π rad. We assume here that this resolution between the two lock points is accomplished perfectly. Then, to compute the average bit-error probability for the hybrid loop for this scenario, one invokes the conditional error probability $P(E;\phi) = 0.5 \text{ erfc}\left(\sqrt{R_d}\cos\phi\right)$ when the loop is locked at zero, i.e., the phase error pdf is governed by $P_0(\phi)$, and the conditional error probability $1 - P(E;\phi) = 1 - 0.5 \text{ erfc}\left(\sqrt{R_d}\cos\phi\right) = P(E;\phi \pm \pi)$ (invert the detected data) when the loop is locked at π rad, i.e., the phase error pdf is governed by $p_\pi(\phi)$. In mathematical terms,

$$P(E) = P_0 \int_{-\pi}^{\pi} 0.5 \text{ erfc}\left(\sqrt{R_d}\cos\phi\right) p_0(\phi)d\phi + P_\pi \int_{-\pi}^{\pi} \left[1 - 0.5 \text{ erfc}\left(\sqrt{R_d}\cos\phi\right)\right] p_\pi(\phi)d\phi \tag{51}$$

For the special case of a 90-deg modulation angle, $P_0 = P_\pi = 1/2$ and $p_0(\phi) = p_\pi(\phi \pm \pi)$, in which case, Eq. (51) simplifies to

$$P(E) = \int_{-\pi}^{\pi} 0.5 \text{ erfc}\left(\sqrt{R_d}\cos\phi\right) p_0(\phi)d\phi = \int_{0}^{\pi} \text{ erfc}\left(\sqrt{R_d}\cos\phi\right) p_0(\phi)d\phi \tag{52}$$

Note that, in principle, the result in Eq. (52) differs from what most researchers have used in the past to evaluate the average error probability performance of BPSK systems with Costas loop synchronization, the latter being given by (see [4], Chapter 6, for example)

$$P(E) = \int_{-\pi/2}^{\pi/2} \text{ erfc}\left(\sqrt{R_d}\cos\phi\right) p(\phi)d\phi \tag{53}$$

where $p(\phi)$ is, as before, the pdf obtained by solution of the Fokker–Planck equation, namely, Eq. (26) or Eq. (27). To see how Eqs. (52) and (53) differ, we substitute Eq. (28) into Eq. (53), which gives

$$P(E) = \int_{0}^{\pi/2} \text{ erfc}\left(\sqrt{R_d}\cos\phi\right) p_0(\phi)d\phi + 2\int_{\pi/2}^{\pi} \left[1 - 0.5 \text{ erfc}\left(\sqrt{R_d}\cos\phi\right)\right] p_0(\phi)d\phi \tag{54}$$

Rewriting Eq. (52) as

$$P(E) = \int_{0}^{\pi/2} \text{ erfc}\left(\sqrt{R_d}\cos\phi\right) p_0(\phi)d\phi + \int_{\pi/2}^{\pi} \text{ erfc}\left(\sqrt{R_d}\cos\phi\right) p_0(\phi)d\phi \tag{55}$$

we see that the difference lies in the way the conditional error probability is handled in the region $\pi/2 \le \phi \le \pi$. Since in this region $0.5 \text{ erfc}\left(\sqrt{R_d}\cos\phi\right) \le 1 - 0.5 \text{ erfc}\left(\sqrt{R_d}\cos\phi\right)$, then $P(E)$ as computed from Eq. (55) will be larger than that value computed from Eq. (54) (the previously used result). For a large loop SNR, the contribution of the second terms in Eqs. (54) and (55) will be small and, thus, this discrepancy will be unnoticeable, which is perhaps the reason it has not previously been identified in practice. Nevertheless, from a theoretical standpoint, it is necessary to point out the difference between the two results.

VIII. Conclusions

We have shown that by making use of the total power available in the received signal for purposes of carrier synchronization, a hybrid loop can provide improved tracking and average bit-error probability performance relative to that achieved by the more conventional Costas loop or phase-locked loop. In assessing the performance of the system, however, one must take into account the fact that, for values of modulation angle larger than a certain critical value, the hybrid loop can lock at both 0- and 180-deg phase error with probabilities dependent on the modulation angle itself. As such, one must either employ differential encoding/decoding or provide a method for resolving this phase ambiguity, such as the inclusion of a unique synchronization word in the data stream. It is also important to properly choose the relative gains in the two arms (discrete carrier and sideband) of the hybrid loop since, depending on the value of the modulation angle, the loop performance can be quite sensitive to these gain settings. Finally, we point out that the actual loop SNR for the hybrid loop, as measured by computer simulation and analytically modeled in this article, is not equal to the sum of the SNRs for the PLL and the Costas loop components, as heretofore suggested in [2].

References

[1] W. C. Lindsey, "Hybrid Carrier and Modulation Tracking Loops," *IEEE Transactions on Communications*, vol. COM-20, no. 1, pp. 53–55, February 1972.

[2] R. Sfeir, S. Aguirre, and W. J. Hurd, "Coherent Digital Demodulation of a Residual Carrier Signal Using IF Sampling," *The Telecommunications and Data Acquisition Progress Report 42-78, April–June 1984*, Jet Propulsion Laboratory, Pasadena, California, pp. 135–142, August 15, 1984.

[3] W. C. Lindsey and M. K. Simon, "Optimum Performance of Suppressed Carrier Receivers With Costas Loop Tracking," *IEEE Transactions on Communications*, vol. COM-25, no. 2, pp. 215–227, February 1977.

[4] W. C. Lindsey and M. K. Simon, *Telecommunication Systems Engineering*, Englewood Cliffs, New Jersey: Prentice-Hall, Inc., 1973.

[5] W. C. Lindsey, *Synchronization Systems in Communication and Control*, Englewood Cliffs, New Jersey: Prentice-Hall, Inc., 1972.

[6] B. Oksendal, *Stochastic Differential Equations: An Introduction With Applications*, Berlin: Springer-Verlag, 1989.

[7] H. Kunita, "Stochastic Partial Differential Equations Connected With Nonlinear Filtering," *Nonlinear Filtering and Stochastic Control*, edited by S. K. Mitter and A. Moro, Berlin: Springer-Verlag, pp. 100–169, 1982.

[8] A. Bensoussan, R. Glowinski, and A. Rascanu, "Approximation of Zakai Equation by the Splitting-Up Method," *Stochastic Systems and Optimization*, edited by J. Zabczyk, Berlin: Springer-Verlag, pp. 257–265, 1989.

Appendix

Steady-State Conditional PDFs

Following the treatment in [6], in this appendix we are primarily interested in synchronous control loops that satisfy stochastic differential equations (SDEs) of the form

$$d\phi(t) = -f(\phi)dt + dB(t), \quad \phi(0) = \phi_0 \tag{A-1}$$

where $\phi(t)$ is a vector[8] in R^d, $f(\cdot)$ is a bounded continuous function from R^d into R^d where d is the order of the loop, and $B(t)$ is a Brownian motion process in R^d with associated power spectral matrix Q. The initial condition ϕ_0 is assumed to have a known pdf, $p_0(\phi)$. It is well known that the pdf $p(\phi, t)$ of the process $\phi(t)$ is the unique solution to the classical forward Kolmogorov equation (FKE):

$$\frac{\partial}{\partial t}p(\phi, t) = Lp(\phi, t), \quad p(\phi, 0) = p_0(\phi) \tag{A-2}$$

where L is the Fokker–Planck operator given by

$$Lp(\phi, t) = \sum_{i=1}^{d}\sum_{j=1}^{d}\frac{q_{ij}}{2}\frac{\partial^2}{\partial\phi_i\partial\phi_j}p(\phi, t) + \sum_{i=1}^{d}\frac{\partial}{\partial\phi_i}\left(f_i(\phi)p(\phi, t)\right) \tag{A-3}$$

where q_{ij} is the (i, j) element of the matrix QQ^T, and $f_i(\phi)$ is the ith component of the vector $f(\phi)$. Suppose that $\phi(t)$ is observed through the observation process $Y(t)$ given by

$$dY(t) = h(\phi)dt + dV(t) \tag{A-4}$$

where $Y(t)$ and $V(t)$ are Brownian motion processes independent of $B(t)$ and ϕ_0, $h(\cdot)$ is an arbitrary function, which, along with its derivatives, is a bounded continuous function from R^d to R^k with $k \leq d$. For simplicity, we assume that $V(t)$ has unit power spectral density. The conditional pdf for the process $\phi(t)$ conditioned on the observation process $\{Y(s) : 0 \leq s \leq t\}$, which we denote by $p_Y(\phi, t)$, is the unique solution of the Zakai equation:

$$dp_Y(\phi, t) = Lp_Y(\phi, t)dt + p_Y(\phi, t)h^T(\phi)dY(t), \quad p(\phi, 0) = p_0(\phi) \tag{A-5}$$

where the superscript T denotes the transpose operation. A derivation of the Zakai equation is given in [7]. One numerical technique for solving Eq. (A-5), the splitting-up method [8], is briefly summarized below. We assume a discrete observation process of the form

$$z(n) = h(\phi(n)) + v(n) \tag{A-6}$$

where $z(n)$ is a discrete representation of $dY(t)$, and $v(n)$ is white noise with unit power spectral matrix. First, we use a uniformly spaced finite-difference scheme on a finite grid to discretize the spatial domain. We obtain a system of stochastic differential equations of the form

[8] To maintain simplicity, we do not introduce a special notation (such as boldface) for vectors.

$$dp_Y(t) = L_h p_Y(t)dt + B_h p_Y(t)dY(t) \tag{A-7}$$

where $p_Y(t) = (p_Y^1(t), \cdots, p_Y^N(t))$ with $p_Y^i(t)$ denoting the conditional pdf at grid point ϕ_i; L_h is the matrix representation of the discretized operator L; and B_h is a diagonal matrix with $h(\phi_i)$ as its diagonal. The splitting-up algorithm (using a Euler backwards scheme) for the numerical integration of the finite dimensional Zakai equation, Eq. (A-7), is given by

$$(I - \Delta t\ L_h)p_{n+1} = \Psi_{n+1}p_n \tag{A-8}$$

where $p_n = p_Y(t_n)$, and Ψ_{n+1} is a diagonal matrix with diagonal elements

$$\psi_i = \exp\left(\frac{\Delta t}{2}(z(n+1) + z(n))h(\phi_i) - \frac{\Delta t}{2}h^2(\phi_i)\right) \tag{A-9}$$

and Δt is the step size for the Euler scheme. Numerical results for a hybrid phase-locked loop are analyzed in Hamdan et al.[9]

For simplicity, we now consider Eq. (A-1) in R^1, which in our application corresponds to a first-order loop. We assume that the corresponding deterministic system has m asymptotically stable equilibrium points, $\{\phi_{l1}, \cdots, \phi_{lm}\}$. That is, $f(\phi_{lk}) = 0$ and $f'(\phi_{lk}) > 0$ for $k = 1, \cdots, m$. Let $p(\phi)$ be the steady-state solution to the associated FPE $LP = 0$. In steady state, we assume that the expected transition time from one (neighborhood) of a stable equilibrium point to another is large enough such that the notion of a steady-state conditional pdf has physical meaning. In this case, we may define the function $p_k(\phi) = p(\phi|\phi \in N(\phi_{lk}))$, where $N(\phi_{lk})$ is a neighborhood of ϕ_{lk}. As a result, there exist constants $P_1, \cdots, P_m$ such that

$$p(\phi) = \sum_{k=1}^{m} P_k p_k(\phi) \tag{A-10}$$

where P_k is the probability of being in $N(\phi_{lk})$ in steady state. Equation (31) is an example of such for $m = 2$. We now follow the treatment in Hamdan et al., where an approximate elliptic partial differential equation for $p_k(\phi)$ is obtained.[10] To this end, consider the observation process defined by Eq. (A-6). The corresponding difference equation for the conditional pdf (with the dependence on k suppressed) is given by Eq. (A-8).

Let us assume that, for some n sufficiently large, we observe the system in $N(\phi_{lk})$ (i.e., the phase is locked at the point ϕ_{lk}). Thus, we may use the approximation

$$\phi(n) = \phi_{lk} + \xi(n), \quad z(n) = h(\phi_{lk} + \xi(n)) + v(n)$$

where $\xi(n)$ is a random deviation of the state from the locked position, and $v(n)$ is the sequence of measurement noise, assumed to be an independent identically distributed (i.i.d.) sequence. In particular, the variance of the measurement noise is assumed to be of the order $\Delta(t)$ ($o(\Delta t)$) uniformly in n. Expanding the observation process about $\xi(n)$, we obtain

[9] K. Hamdan, S. Hinedi, and M. Simon, op cit.

[10] Ibid.

$$\frac{\Delta t}{2}(z(n+1)+z(n)) = \Delta t\; h(\phi_{lk}) + \lambda_n \tag{A-11}$$

where

$$\lambda_n = \frac{\Delta t}{2}\left(h'(\phi_{lk})(\xi(n)+\xi(n+1)) + v(n+1) + v(n)\right) + o\left(\Delta t \xi(n)^2\right)$$

Substituting Eq. (A-11) into Eq. (A-9) and expanding the exponential term, Eq. (A-8) becomes

$$(I - \Delta t\; L_h)\, p_{n+1} = Ap_n + \lambda_n A p_n \tag{A-12}$$

where I is the identity matrix and A is a diagonal matrix with diagonal entries

$$\exp\left(\Delta t\; h(\phi_{lk})h(\phi_i) - \frac{\Delta t}{2}h^2(\phi_i)\right)$$

Under some mild conditions, it is shown in Hamdan et al. that if for n arbitrarily large, the system remains locked at the equilibrium point ϕ_{lk}, then λ_n (in steady state) converges to a random variable λ with variance $o(\Delta t)$.[11] By letting n approach infinity in Eq. (A-12), we obtain the following equation for the steady-state conditional pdf:

$$A^{-1}\,(I - \Delta t\; L_h - A)\, p = \lambda p \tag{A-13}$$

where λ is a random variable with $o(\Delta t)$ variance. By letting $\Delta t = 1$, we obtain the infinite dimensional analogue of the matrix equation, Eq. (A-13):

$$g(\phi, \phi_{lk}) L p(\phi) + (1 + \lambda - g(\phi, \phi_{lk}))\, p(\phi) = 0 \tag{A-14}$$

where L is the Fokker–Planck operator defined in Eq. (A-3), and

$$g(\phi, \phi_{lk}) = \exp\left(\frac{1}{2}h^2(\phi) - h(\phi_{lk})h(\phi)\right) \tag{A-15}$$

[11] Ibid.